

# Inhibition of $\gamma$ -Secretase Activity by a Monoclonal Antibody against the Extracellular Hydrophilic Loop of Presenilin 1

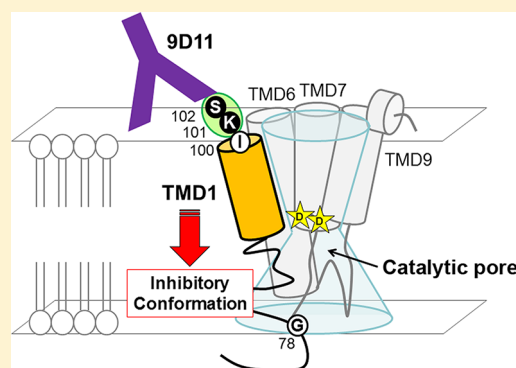
Shizuka Takagi-Niidome,<sup>†</sup> Satoko Osawa,<sup>†</sup> Taisuke Tomita,<sup>\*,†,‡</sup> and Takeshi Iwatsubo<sup>†,‡,§</sup>

<sup>†</sup>Department of Neuropathology and Neuroscience, Graduate School of Pharmaceutical Sciences, The University of Tokyo, Tokyo 113-0033, Japan

<sup>‡</sup>Core Research for Evolutional Science and Technology, Japan Science and Technology Agency, Tokyo 113-0033, Japan

<sup>§</sup>Department of Neuropathology, Graduate School of Medicine, The University of Tokyo, Tokyo 113-0033, Japan

**ABSTRACT:** Presenilin 1 (PS1) comprises a catalytic subunit of  $\gamma$ -secretase, which is an intramembrane-cleaving protease responsible for generation of amyloid- $\beta$  peptides as well as Notch cleavage, the latter being implicated in cancer. We have shown that transmembrane domains (TMDs) 1, 6, 7, and 9 of PS1 form the “catalytic pore” structure within the membrane for intramembrane proteolysis. Here we report a novel monoclonal antibody 9D11, which directly recognizes the TMD1-proximal residues in the hydrophilic loop region. Intriguingly, 9D11 inhibited the  $\gamma$ -secretase activity irrespective of the binding of known  $\gamma$ -secretase inhibitors and abolished Notch signaling-dependent cancer cell viability. Our data suggest that the juxtamembrane region of TMD1 of PS1 is a novel molecular target for the mechanism-based inhibition of  $\gamma$ -secretase and the development of the anticancer drug.



Intramembrane proteolysis is an atypical hydrolysis of peptide bonds within the lipid bilayer. Several lines of evidence suggest that this atypical cleavage is involved in numerous biological processes encompassing all branches of life. So far, four families of intramembrane-cleaving proteases have been discovered: rhomboid, site-2 protease (S2P), signal peptide peptidase, and  $\gamma$ -secretase.<sup>1</sup>  $\gamma$ -Secretase is a key enzyme in the production of amyloid- $\beta$  peptide (A $\beta$ ), a major component of senile plaques in the brains of patients with Alzheimer's disease.<sup>2,3</sup> Moreover,  $\gamma$ -secretase mediates proteolysis-dependent signaling of several type I membrane proteins, including the Notch receptor, which is involved in the development of cancer.<sup>3,4</sup> Thus, rational design of  $\gamma$ -secretase inhibitors (GSIs) based on the molecular mechanism of  $\gamma$ -secretase would pave the way for the development of novel drugs.<sup>5</sup> However, structural analysis of  $\gamma$ -secretase has not been fully achieved; this atypical protease is comprised of at least four transmembrane proteins: nicastrin (Nct), anterior pharynx defective-1 (Aph-1), presenilin enhancer-2 (Pen-2), and PS1, the latter representing the catalytic subunit.<sup>3,6</sup> In contrast, structural analyses of rhomboid and S2P family intramembrane proteases have revealed that membrane-embedded active sites of these proteases are indeed hydrated within the intramembrane cavity or channel-like structure.<sup>7</sup> These data suggest that hydrolysis of transmembrane helices occurs within the membrane. However, the molecular and structural bases of the recognition and incorporation of the hydrophobic substrates remain unknown.

We have been applying the substituted cysteine accessibility method (SCAM) to gain insight into the structure of PS1 in a

membrane-embedded state. The SCAM has been reiteratively used to obtain structural information about various multipass membrane proteins in a functional state, by covalently modifying the introduced cysteine (Cys) residues using sulfhydryl reagents.<sup>8–10</sup> Using the SCAM, we and others have revealed that PS1 harbors a hydrophilic “catalytic pore” formed by TMD1, -6, -7, and -9.<sup>11–15</sup> This suggests that the hydrophilic milieu around the active site located within the lipid bilayer is a common structure across intramembrane-cleaving proteases. In addition, upon incubation of GSI, we identified the movement of TMD1 of PS1 [i.e., from glycine 78 (G78) to isoleucine 100 (I100)] downward to the cytosolic side, which was evidenced by specific changes in the hydrophilicity of the microenvironment of amino acid residues located at the borders of TMD1 (i.e., G78 and I100) in the SCAM.<sup>15</sup> Here we developed rat monoclonal antibody (mAb) 9D11 against the juxtamembrane region of TMD1. Intriguingly, 9D11 treatment reduced the  $\gamma$ -secretase activity as well as the extent of growth of the cancer cell line. However, a photoaffinity labeling experiment revealed that the binding mode of 9D11 is totally distinct from that of the small compound-based known GSIs. Our data indicate that the juxtamembrane region of TMD1 might be a novel target domain for the development of therapeutics against cancer caused by an abnormal upregulation of  $\gamma$ -secretase activity.<sup>3,4</sup>

**Received:** September 13, 2012

**Revised:** December 4, 2012

**Published:** December 4, 2012



## ■ EXPERIMENTAL PROCEDURES

**Production and Purification of Anti-Hydrophilic Loop 1 of PS1 mAbs.** All experimental procedures were performed in accordance with the guidelines for animal experiments of The University of Tokyo. Glutathione S-transferase (GST) fusion protein containing residues K101–M139 of PS1 [GST hydrophilic loop 1 (HL1)] was purified using glutathione Sepharose 4B (GE Healthcare). Eight-week-old WKY/Izm rats were purchased from Japan SLC and immunized with 100  $\mu$ g of purified GST-HL1 in Freund's complete adjuvant (Sigma), via footpad injection.<sup>16</sup> One month after the first boost, immunized rats were tail bled and serum titers were checked using an enzyme-linked immunosorbent assay (ELISA) (see below) and reboosted. B cells obtained from the iliac and inguinal lymph nodes were fused with a PAI myeloma cell that was a kind gift of H. Arai (The University of Tokyo). The hybridoma cells were cultured in HAT selection medium [GIT medium (Wako Pure Chemical Industries) containing 5% FBS (Hyclone), 5% NCTC109 (Invitrogen), 1% nonessential amino acids (Invitrogen), 1% penicillin-streptomycin-glutamine (Invitrogen), purified interleukin-6, 100  $\mu$ M hypoxanthine, 0.4  $\mu$ M aminopterin, and 16  $\mu$ M thymidine]. The hybridoma supernatants were screened for antibodies using an ELISA with a KLH-conjugated synthetic peptide encoding K101–T124 of PS1 (BEX, Co. Ltd.). For the purification of mAbs, hybridoma cells were cultured in GIT medium containing 5% NCTC109, 1% nonessential amino acids, and 1% penicillin-streptomycin-glutamine. mAbs in cultured media were purified using the MAbTrap Kit (GE Healthcare) according to the manufacturer's instructions. Rat IgG used as the control IgG was purchased from Sigma-Aldrich Japan. Purified mAb was stored at  $-80^{\circ}\text{C}$  before use.

**ELISA System for mAb Screening and Epitope Mapping.** KLH-conjugated peptides and sequential peptides for epitope mapping were purchased from BEX and Sigma-Aldrich Japan, respectively. Peptides (10  $\mu$ g/mL) or GST fusion proteins (1  $\mu$ g/mL) in PBS were added to a 96-well plate and incubated overnight at  $4^{\circ}\text{C}$ . The coated plates were blocked with PBS containing 3% bovine serum albumin and 0.1% sodium azide. The hybridoma cell culture supernatant or purified mAb in PBS was added and the mixture incubated overnight at  $4^{\circ}\text{C}$ . After the wells had been washed four times with PBS, anti-rat IgG coupled to horseradish peroxidase (GE Healthcare) was added at a dilution of 1:2000 and incubated at room temperature for 2 h. The wells were washed six times with PBS and detected with a TMB microwell peroxidase substrate system (Kirkegaard & Perry Laboratories Inc.), and the optical density at 450 nm was measured.

**Plasmid Construction, Cell Culture, Transfection, and Retroviral Infection.** For the generation of GST-HL1, cDNAs encoding HL1 of PS1 were inserted into pGEX-6P-1 (GE Healthcare). cDNAs encoding PS1 and Cys-less PS1 were inserted into pMXs-puro as previously described.<sup>11,17</sup> Mutant forms of PS1 were generated using a long polymerase chain reaction-based protocol. Construction of SC100 fused with the gal4 sequence (SC100-gal4) in pcDNA3.1/Hyg(+), EGFP in pcDNA3, UAS-luc in pGL3(r2.2), SPC99gvp-6myc in pMXs-puro, NAE-6myc in pLPCX, UAS-firefly luciferase in pMXs-EGFP, and TP1-renilla luciferase in pMXs-II was conducted as previously described.<sup>17–19</sup> Maintenance of *Psen1*<sup>−/−</sup>/*Psen2*<sup>−/−</sup> double-knockout embryonic fibroblast (DKO), Plat-E, HEK293, HeLa, and A549 cells, retroviral infection, and

generation of stable infectant pools were conducted as described previously.<sup>11,12,15,17,19–22</sup>

**Antibodies, Immunochemical Analyses, and  $\gamma$ -Secretase Assays.** Polyclonal antibodies G1Nr5, G1L3, and PNT3 against the N-terminus of PS1, the cytoplasmic loop region of PS1, and the N-terminal region of Pen-2, respectively, have been previously described.<sup>18,23,24</sup> C502 is a rabbit polyclonal antibody against recombinant protein encoding the C-terminal domain of APP (residues 646–695) with a C-terminal FLAG-myc-6xHis tandem tag. Anti-Nct monoclonal antibody A5226A, which recognizes an active form of Nct, was described previously.<sup>22</sup> The anti-PS1NT antibody was kindly provided by G. Thinakaran (The University of Chicago, Chicago, IL).<sup>25</sup> Other antibodies were purchased from Cell Signaling Technology [anti-cleaved Notch1 (V1744)], Covance [anti-Aph-1aL (O2C2)], Immuno-Biological Laboratories [anti-human APP (C)], or Sigma [anti-Nct (N1660) and anti- $\alpha$ -tubulin (DM1A)]. Membrane fractionation, immunoblot analysis, immunoprecipitation of 3-[(3-cholamidopropyl)-dimethylammonio]-2-hydroxy-1-propanesulfonate (CHAP-SO)-solubilized lysates, immunocytochemistry, the in vitro  $\gamma$ -secretase assay, the cell-free  $\gamma$ -secretase assay, and quantitation of A $\beta$  by two-site ELISAs were performed as previously described.<sup>26–32</sup> HEK293/SC100-gal4 cells and #5/DKO reporter cells for A $\beta$  and luciferase assays, respectively, were plated on 96-well plates 24 h before the addition of the designated concentration of antibodies or DAPT (50  $\mu$ M). The treated cell lysates were subjected to the luciferase measurement as previously described.<sup>18</sup> In the cell viability assay using A549, cells were plated in 96-well plates (5000 cells per well, 100  $\mu$ L) 24 h before the addition of DAPT or mAb. After incubation for 96 h, 10  $\mu$ L of Alamar Blue (Serotec, Oxford, U.K.) was added to each well and incubated for 3 h at  $37^{\circ}\text{C}$ . Cell viability was calculated from the fluorescence value for Alamar Blue.<sup>22</sup>

**Compounds, Substituted Cysteine Accessibility Method (SCAM), and Photoaffinity Labeling.** N-biotinaminoethyl methanethiosulfonate (MTSEA-biotin) (Toronto Research Chemicals, Toronto, ON) was dissolved in DMSO at 200 mM and stored at  $-80^{\circ}\text{C}$  until use. 31C and 31C-Bpa were kindly provided by N. Umezawa and T. Higuchi (Nagoya City University, Aichi, Japan).<sup>18</sup> Peptide 11 (pep11) and pep11-Bt were purchased from Ito Life Science and BEX, respectively. N-[N-(3,5-Difluorophenacetyl)-L-alanyl]-L-(S)-phenylglycine tert-butyl ester (DAPT) and DAP-BpB were gifts from T. Fukuyama (The University of Tokyo).<sup>33</sup> In SCAM analysis, microsome pellets were resuspended in PBS and incubated with 9D11 or rat IgG (1  $\mu$ g/mL) for 30 min at room temperature before being labeled with MTSEA-biotin. Further details about SCAM analysis have been previously described.<sup>11</sup> Photoaffinity labeling experiments were performed using microsome fractions from DKO cells expressing wild-type (wt) PS1 as previously described.<sup>17,18,34</sup>

## ■ RESULTS

**9D11 Recognized the Juxtamembranous Residues of HL1 Proximal to TMD1 of PS1.** We developed rat mAbs<sup>16</sup> targeting the juxtamembrane region at the extracellular side of TMD1 using GST fused to residues K101–M139 of PS1 corresponding to HL1. We isolated mAb clone 9D11 of the IgG2b isotype that specifically reacted with synthetic peptides that included K101 or S102; the latter results suggest that the epitope of 9D11 sits at the most N-terminal residues of PS1



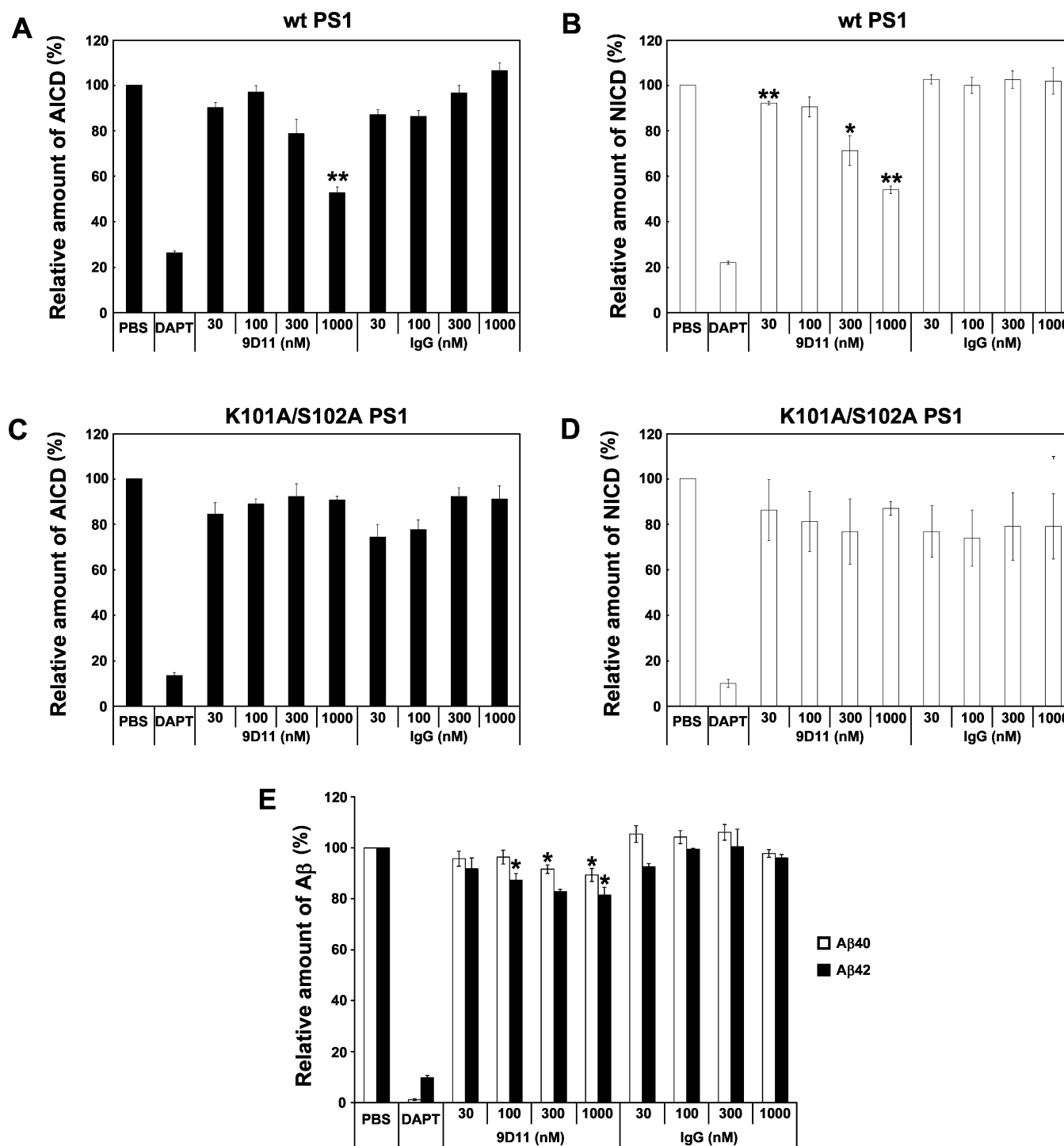


**Figure 2.** Effects of 9D11 on the  $\gamma$ -secretase activity of living cells. (A and B) Effects of 9D11 on the production ratio of AICD and NICD in a cell-based  $\gamma$ -secretase assay. DKO cells expressing APP and Notch luciferase reporters were transiently transfected with wt PS1. AICD (A) and NICD (B) levels are indicated by black and white bars, respectively ( $n = 3$ ; mean  $\pm$  SEM; \* $p < 0.05$ ; \*\* $p < 0.01$  against control rat IgG at each concentration). Values for DAPT (10  $\mu$ M) or IgG are shown as controls. (C and D) Effects of 9D11 on K101A/S102A PS1-containing  $\gamma$ -secretase activity in a cell-based  $\gamma$ -secretase assay using reporter cells transfected with K101A/S102A PS1 ( $n = 3$ ; mean  $\pm$  SEM). Values for DAPT (10  $\mu$ M) or IgG are shown as controls. (E) Effects of 9D11 on the production ratio of A $\beta$  in a cell-based  $\gamma$ -secretase assay. Secreted A $\beta$  in cultured media was analyzed by sandwich ELISAs ( $n = 3$ ; mean  $\pm$  SEM; \* $p < 0.05$  against control rat IgG at each concentration).

survival of A549 cells as previously reported.<sup>22</sup> Furthermore, 9D11 significantly reduced the viability of A549 cells, which was not affected by rat IgG (Figure 3). These data support our notion that 9D11 inhibits the  $\gamma$ -secretase on the surface of living cells and inhibits the intramembrane cleaving activity by targeting residues K101 and S102 of PS1.

Next we examined the molecular effect of 9D11. We did not observe any significant change in the localization of endogenous Nct in HeLa cells treated with 9D11, which was probed by monoclonal antibody A5226A that recognizes an active  $\gamma$ -secretase complex<sup>22</sup> (Figure 4A). Moreover, 9D11 treatment did not alter the levels of the N-terminal fragment



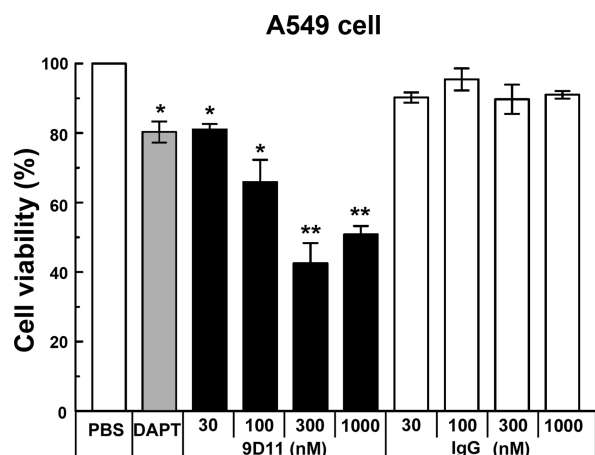


**Figure 3.** Effect of 9D11 on the viability of A549 cells. A549 cells were treated with 9D11, rat IgG, or DAPT (50  $\mu$ M), and the cell viability was measured by the Alamar Blue assay ( $n = 3$ ; mean  $\pm$  SEM; \* $p < 0.05$ ; \*\* $p < 0.01$  against control rat IgG at each concentration or DMSO for DAPT).

that represents an active form of PS1 (Figure 4B),<sup>6</sup> suggesting that 9D11 did not affect the localization or the amount of the active  $\gamma$ -secretase by direct targeting of the enzyme. To gain further insight into the mechanism of the inhibitory effect of 9D11, we performed cross-competition experiments of the photoaffinity labeling of PS1 by small compound GSI-based probes.<sup>18</sup> We utilized three photoaffinity probes that target different molecular sites within PS1: 31C-Bpa for the catalytic site,<sup>37</sup> pep11-Bt for the initial substrate-binding site,<sup>38</sup> and DAP-BpB for the transit path that connects the substrate-binding and catalytic sites of the  $\gamma$ -secretase.<sup>39</sup> Preincubation of 9D11 showed no change in the binding of the photoprobe to PS1 (Figure 4C), suggesting that inhibition of the  $\gamma$ -secretase activity by 9D11 was achieved without affecting the structural integrity of the enzymatically functional sites within PS1. In addition, 9D11 failed to inhibit the intrinsic  $\gamma$ -secretase activity under a CHAPSO-solubilized condition (Figure 4D–F), while the level of AICD production was significantly decreased by 9D11 under detergent-free conditions (Figure 4G,H). These results raise the possibility that the membrane-embedded structure of PS1 is required for the inhibitory activity of 9D11.

To test whether the binding of 9D11 affects the structure of PS1, we applied SCAM analysis, in which the water accessibility of each amino acid residue was evaluated by the efficiency of labeling of MTSEA-biotin with each substituted cysteine residue.<sup>11,12,15</sup> Using this method, we have previously shown that small compound GSIs (i.e., L-685,458, pep15, and DAPT) caused the stabilization of the position of TMD1 that was evidenced by the coordinated reciprocal changes in the reactivity of G78C and I100C to MTSEA-biotin. Intriguingly, the labeling efficiency of G78C was increased, whereas that of I100C was decreased, by the preincubation with 9D11, in a manner similar to that observed with GSIs (Figure 5A).<sup>15</sup> These data indicate that the binding of mAb 9D11 to the juxtamembranous residues at the TMD1–HL1 border caused a structural change similar to that induced by known GSIs (Figure 5B). Moreover, 9D11 did not have any effects on the labeling efficiencies of E71C at the N-terminal extracellular domain of TMD1 and L383C in the catalytic pore. Notably, the hydrophilicity of L383C was decreased by L-685,458 and DAPT,<sup>11</sup> suggesting the local effect of 9D11 on the TMD1

positioning in the membrane. Taken together, our data suggest that 9D11 functions as an allosteric mAb that inhibits the  $\gamma$ -secretase activity in situ via stabilization of PS1 structure as an inhibitory conformation within the membrane.

## DISCUSSION

To date, the correlation of structural dynamics with the enzymatic activity of PS/ $\gamma$ -secretase has never been achieved. In contrast, the structural dynamics of the rhomboid protease has been analyzed, and the motion of L1 loop and TMD5, the latter being closely located to the catalytic site, has been implicated in the gating of lateral substrate entry.<sup>40,41</sup> These reports suggest that the dynamic motion of the TMD and connecting loop would be critical for the proteolysis by intramembrane-cleaving proteases. Here we identified a mAb 9D11 targeting juxtamembrane residues at the TMD1–HL1 border of PS1 as an inhibitory antibody against  $\gamma$ -secretase. Using SCAM analysis, we have found that 9D11 caused the structural change of TMD1 in a manner similar to that of GSI treatment, while the binding sites of these compounds are distinct<sup>15</sup> (see Figure 4C). These data strongly support our notion that the TMD1–HL1 border is involved in the intramembrane-cleaving mechanism.

Biochemical studies revealed that all GSIs investigated so far target PS.<sup>5</sup> However, no inhibitory antibody against PS was reported, while some anti-Nct antibodies have been identified as neutralizing mAbs.<sup>22,42,43</sup> 9D11 is the first mAb targeting PS1 that regulates the  $\gamma$ -secretase activity. We found that K101 and S102 comprise the epitope of 9D11. These residues were conserved only in vertebrates, not in other species. Also, alanine substitutions of these residues did not deactivate the  $\gamma$ -secretase activity, suggesting that these residues are not essential for  $\gamma$ -secretase function. In contrast, our SCAM analysis revealed that 9D11 affected the water accessibility of the juxtamembrane residues of TMD1. Importantly, we have previously reported that the hydrophilicity of the TMD1 border was altered by GSIs.<sup>15</sup> Notably, the position of the TMD in the membrane is critical for the gating of several membrane-embedded channel/pore structures.<sup>44–47</sup> Moreover, recently, X-ray crystallographic analyses of the A<sub>2A</sub> adenosine receptor as well as the  $\beta$ 2 adrenergic receptor bound with antibody fragments were reported.<sup>48,49</sup> These antibody fragments stabilized the receptor structure in inactive and active states irrespective of ligand binding. Intriguingly, these antibodies targeted the TMD–HL border from the cytosolic side of the receptors, thereby allosterically affecting the structure of the ligand binding sites at the luminal side. Thus, it is plausible that the position of TMD1 in the membrane is affected by 9D11 in a manner similar to that of GSIs, leading to the loss of the  $\gamma$ -secretase activity by stabilization of the PS1 conformation as an inhibitory state (Figure 5B). However, we are unable to exclude the possibility that the steric hindrance effect of 9D11 is also involved in the inhibitory mechanism. Nevertheless, this report supports the view that the activity of transmembrane proteins would be regulated by allosteric modulation of the conformation of TMDs.

Here we show that 9D11 inhibits the  $\gamma$ -secretase activity in cultured cells, as well as the viability of cancer cells. These data suggest that the juxtamembrane region of TMD1 is a novel therapeutic target for the development of the treatments against some types of cancer, in which Notch signaling is required for proliferation. However, the use of 9D11 for therapeutics against Alzheimer's disease may not be directly feasible, as penetration

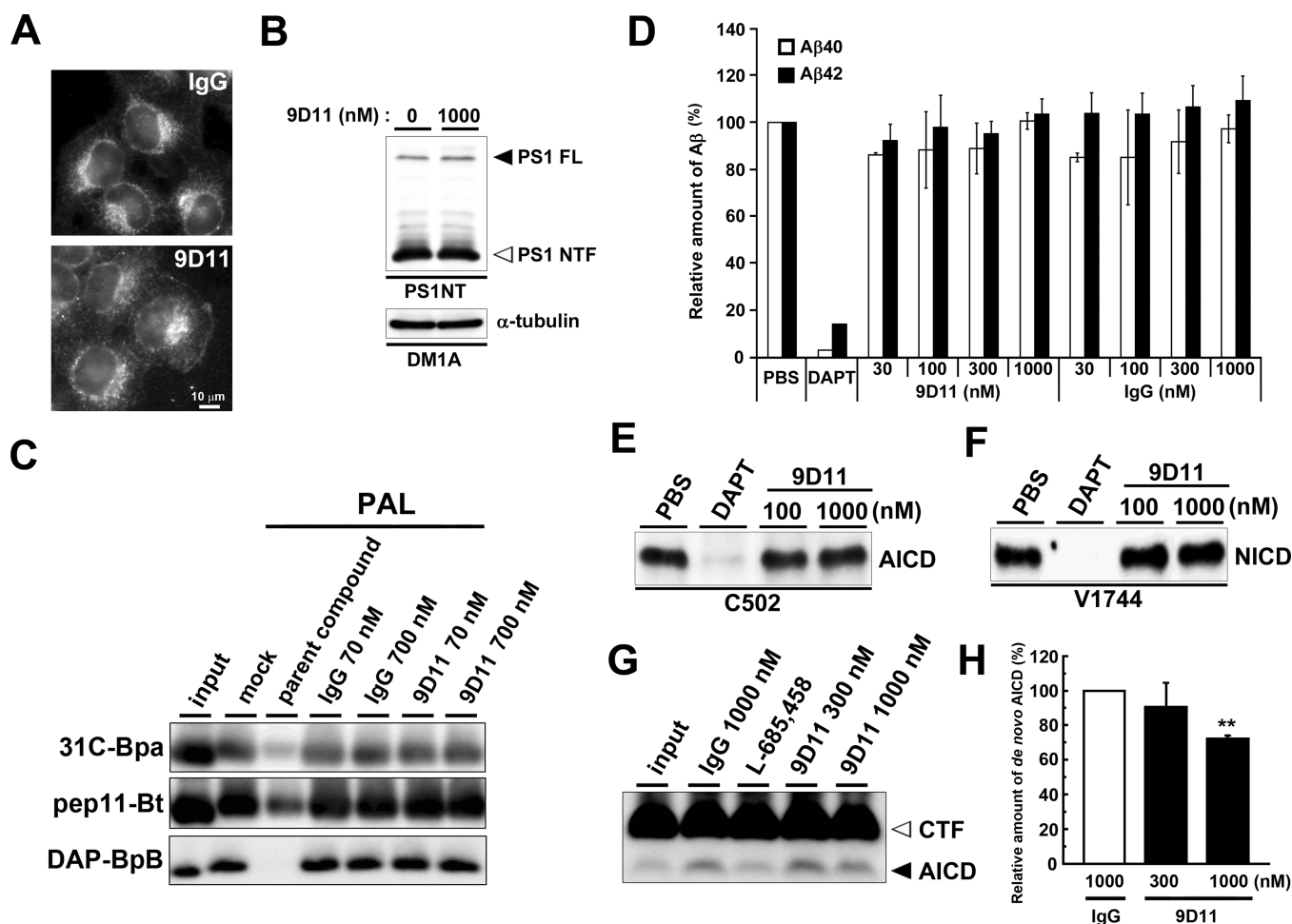


**Figure 4.** Mode of action of the inhibitory effect of 9D11. (A) Immunocytochemical analysis of HeLa cells treated with 9D11 or rat IgG (1  $\mu$ M) for 24 h. Endogenous Nct was visualized by A5226A. (B) Effect of 9D11 on the level of expression of PS1 in DKO cells expressing wt PS1. (C) Competition assay against photoaffinity labeling (PAL) with 31C-Bpa, pep11-Bt, and DAP-BpB in the presence of rat IgG or 9D11. 31C, pep11, and DAPT were used as parent compounds for labeling with 31C-Bpa, pep11-Bt, and DAP-BpB, respectively. The biotinylated PS1 NTF was detected by immunoblotting analysis using anti-PS1NT. (D–F) Effect of 9D11 in the *in vitro*  $\gamma$ -secretase assay. Membranes of DKO cells expressing wt PS1 were solubilized with CHAPSO and co-incubated with recombinant substrate C100-FmH (D and E) or N102-FmH (F)<sup>27</sup> in the presence of 9D11. De novo A $\beta$  generation was analyzed by a sandwich ELISA ( $n = 3$ ; mean  $\pm$  SEM) (D). AICD (E) and NICD (F) production were detected by using antibodies indicated below the panels. (G and H) Effect of 9D11 in the cell-free  $\gamma$ -secretase assay. Membranes from HeLa cells were incubated with rat IgG, L-685,458 (10  $\mu$ M), or 9D11 under detergent-free conditions. De novo AICD generation and retained CTF were detected by anti-APP(C). The quantitation of de novo AICD levels is shown (H) ( $n = 3$ ; mean  $\pm$  SEM; \*\* $p < 0.01$  against control rat IgG).

of the blood–brain barrier by mAb is quite poor, and Notch signaling was also abolished by this mAb. Moreover, the inhibitory activity against A $\beta$  generation was lower than that for AICD/NICD generation (Figure 2). This result would support the previous notion that major subcellular compartments for A $\beta$  and ICD generation are distinct.<sup>35</sup> Importantly, AICD can be released from both C83 and C99 of APP, which are generated by  $\alpha$ -secretase at the cell surface and  $\beta$ -secretase at the endosomal compartment, respectively. Thus, it would be plausible that 9D11 preferentially targets the  $\gamma$ -secretase complex at the cell surface, although we failed to probe 9D11-bound PS1 by conventional immunocytochemistry (data not shown). Alternatively, 9D11 is ineffective with or dissociates from PS1 at the endosomal compartment, where BACE1 generates C99. Nevertheless, modification of 9D11 as a probe for active PS1 would reveal a novel molecular aspect of  $\gamma$ -secretase-mediated cleavage. In addition, we found that PS1/K101A specifically inhibited APP cleavage, while NICD production was retained. We have reported a similar

substrate-selective activity in cells expressing PS1/F86C, suggesting that TMD1 is a critical domain for substrate selectivity.<sup>15</sup> Thus, molecular engineering of 9D11 or selective targeting of TMD1 may lead to the generation of substrate-specific modulatory mAbs. Moreover, the effect of 9D11 on the generation of p3 and N $\beta$ , which are derived from C83 and Notch proteins, respectively, by  $\gamma$ -secretase-mediated cleavage, would provide mechanistic insight into the substrate recognition by the  $\gamma$ -secretase. In conclusion, identification of 9D11 as an inhibitory mAb strengthened our hypothesis that TMD1 of PS1 plays an important role(s) in the catalytic activity in the substrate cleaving process. Further integrated analysis (i.e., X-ray crystallography and molecular dynamics simulation) will facilitate our understanding of the motion–activity relationships of PS1.

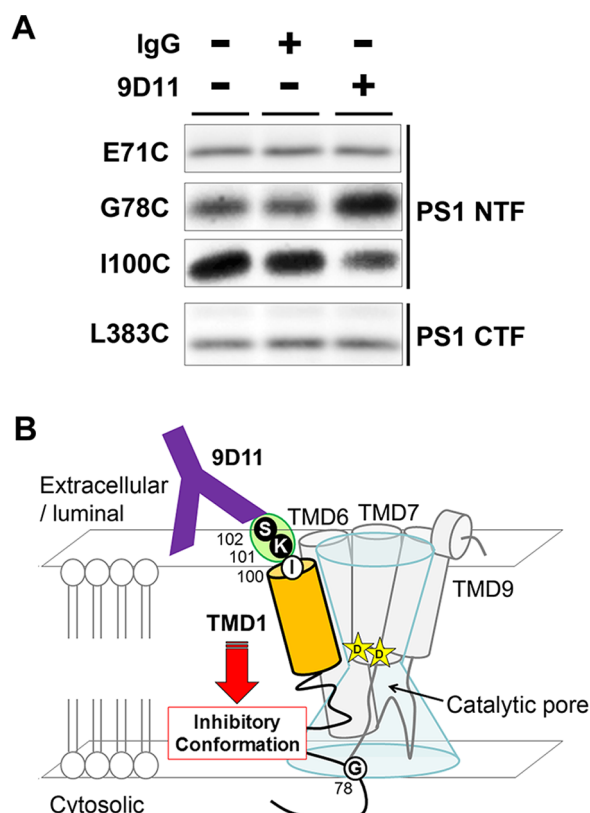


**Figure 5.** Effect of 9D11 on the vertical motion of TMD1 of PS1. (A) SCAM analysis of Cys-less PS1 carrying the E71C, G78C, I100C, or L383C mutation. Labeling by MTSEA-biotin was conducted after preincubation with 9D11 or rat IgG (70 nM). Labeled proteins were precipitated with streptavidin sepharose and detected by the anti-PS1NT antibody and GIL3 for PS1 NTF and CTF, respectively. Note that the hydrophilicities of G78 and I100 are simultaneously affected by 9D11 treatments. (B) Effect of 9D11 on PS1 structure. 9D11 targeting K101 and S102 (in green circles) decreased the  $\gamma$ -secretase activity by stabilizing TMD1 at the downward location in the membrane in a manner similar to that of GSIs. G78 and I100 used for SCAM analysis are indicated in white circles.

## AUTHOR INFORMATION

### Corresponding Author

\*Department of Neuropathology and Neuroscience, Graduate School of Pharmaceutical Sciences, The University of Tokyo, Tokyo 113-0033, Japan. Phone: +81-3-5841-4868. E-mail: taisuke@mol.f.u-tokyo.ac.jp.

### Author Contributions

S.T.-N. and T.T. designed the research. S.T.-N. and S.O. performed biochemical experiments. S.T.-N., T.T., and T.I. wrote the paper. All authors have given approval to the final version of the manuscript.

### Funding

This work was supported in part by grants-in-aid for Young Scientists (S) from the Japan Society for the Promotion of Science (JSPS) (T.T.), by the Targeted Proteins Research Program of the Japan Science and Technology Corp. (JST) (T.T. and T.I.), and by Core Research for Evolutional Science and Technology of JST (T.T. and T.I.). S.T.-N. is a research fellow of JSPS.

### Notes

The authors declare no competing financial interests.

## ACKNOWLEDGMENTS

We thank Drs. B. De Strooper (Katholieke Universiteit Leuven, Leuven, Belgium), R. Kopan (Washington University at St. Louis, St. Louis, MO), U. Strobl (Helmholtz Zentrum Munchen, Munich, Germany), T. Kitamura, H. Arai, and T. Fukuyama (The University of Tokyo), N. Umezawa and T. Higuchi (Nagoya City University, Nagoya, Japan), K. I. Nakayama (Kyushu University, Fukuoka, Japan), and G. Thinakaran (The University of Chicago) for valuable reagents, Takeda Pharmaceutical Co. (Osaka, Japan) for the  $A\beta$  ELISA, J. Takagi (The University of Osaka, Osaka, Japan) for productive discussions, and our current and previous laboratory members for helpful discussions and technical assistance.

## ABBREVIATIONS

$A\beta$ , amyloid- $\beta$  peptide; AICD, APP intracellular domain; Aph-1, anterior pharynx defective-1; DKO, *Psен1*<sup>-/-</sup>/*Psен2*<sup>-/-</sup> double-knockout embryonic fibroblast; ELISA, enzyme-linked immunosorbent assay; GSI,  $\gamma$ -secretase inhibitor; HL, hydrophilic loop; Nct, nicastrin; NICD, Notch intracellular domain; mAb, monoclonal antibody; mt, mutant; MTSEA-biotin, *N*-biotinaminoethyl methanethiosulfonate; Pen-2, presenilin enhancer-2; PS, presenilin; S2P, site-2 protease; SCAM, substituted cysteine accessibility method; SEM, standard error of the mean; TMD, transmembrane domain; wt, wild-type.

## REFERENCES

- (1) Wolfe, M. S., and Kopan, R. (2004) Intramembrane proteolysis: Theme and variations. *Science* 305, 1119–1123.
- (2) Holtzman, D. M., Morris, J. C., and Goate, A. M. (2011) Alzheimer's disease: The challenge of the second century. *Sci. Transl. Med.* 3, 77sr71.
- (3) De Strooper, B., Iwatsubo, T., and Wolfe, M. S. (2012) Presenilins and  $\gamma$ -Secretase: Structure, Function, and Role in Alzheimer Disease. *Cold Spring Harbor Perspect. Med.* 2, a006304.
- (4) Pannuti, A., Foreman, K., Rizzo, P., Osipo, C., Golde, T., Osborne, B., and Miele, L. (2010) Targeting Notch to target cancer stem cells. *Clin. Cancer Res.* 16, 3141–3152.
- (5) Tomita, T. (2009) Secretase inhibitors and modulators for Alzheimer's disease treatment. *Expert Rev. Neurother.* 9, 661–679.
- (6) Takasugi, N., Tomita, T., Hayashi, I., Tsuruoka, M., Niimura, M., Takahashi, Y., Thinakaran, G., and Iwatsubo, T. (2003) The role of presenilin cofactors in the  $\gamma$ -secretase complex. *Nature* 422, 438–441.
- (7) Erez, E., Fass, D., and Bibi, E. (2009) How intramembrane proteases bury hydrolytic reactions in the membrane. *Nature* 459, 371–378.
- (8) Kaback, H. R., Sahin-Toth, M., and Weinglass, A. B. (2001) The kamikaze approach to membrane transport. *Nat. Rev. Mol. Cell Biol.* 2, 610–620.
- (9) Karlin, A., and Akabas, M. H. (1998) Substituted-cysteine accessibility method. *Methods Enzymol.* 293, 123–145.
- (10) Seal, R. P., Leighton, B. H., and Amara, S. G. (1998) Transmembrane topology mapping using biotin-containing sulphydryl reagents. *Methods Enzymol.* 296, 318–331.
- (11) Sato, C., Morohashi, Y., Tomita, T., and Iwatsubo, T. (2006) Structure of the catalytic pore of  $\gamma$ -secretase probed by the accessibility of substituted cysteines. *J. Neurosci.* 26, 12081–12088.
- (12) Sato, C., Takagi, S., Tomita, T., and Iwatsubo, T. (2008) The C-terminal PAL motif and transmembrane domain 9 of presenilin 1 are involved in the formation of the catalytic pore of the  $\gamma$ -secretase. *J. Neurosci.* 28, 6264–6271.
- (13) Tolia, A., Chavez-Gutierrez, L., and De Strooper, B. (2006) Contribution of presenilin transmembrane domains 6 and 7 to a water-containing cavity in the  $\gamma$ -secretase complex. *J. Biol. Chem.* 281, 27633–27642.



- (14) Tolia, A., Horre, K., and De Strooper, B. (2008) Transmembrane domain 9 of presenilin determines the dynamic conformation of the catalytic site of  $\gamma$ -secretase. *J. Biol. Chem.* 283, 19793–19803.
- (15) Takagi, S., Tominaga, A., Sato, C., Tomita, T., and Iwatsubo, T. (2010) Participation of transmembrane domain 1 of presenilin 1 in the catalytic pore structure of the  $\gamma$ -secretase. *J. Neurosci.* 30, 15943–15950.
- (16) Tanaka, M., Kishi, Y., Takanezawa, Y., Kakehi, Y., Aoki, J., and Arai, H. (2004) Prostatic acid phosphatase degrades lysophosphatidic acid in seminal plasma. *FEBS Lett.* 571, 197–204.
- (17) Watanabe, N., Tomita, T., Sato, C., Kitamura, T., Morohashi, Y., and Iwatsubo, T. (2005) Pen-2 is incorporated into the  $\gamma$ -secretase complex through binding to transmembrane domain 4 of presenilin 1. *J. Biol. Chem.* 280, 41967–41975.
- (18) Imamura, Y., Watanabe, N., Umezawa, N., Iwatsubo, T., Kato, N., Tomita, T., and Higuchi, T. (2009) Inhibition of  $\gamma$ -secretase activity by helical  $\beta$ -peptide foldamers. *J. Am. Chem. Soc.* 131, 7353–7359.
- (19) Watanabe, N., Takagi, S., Tominaga, A., Tomita, T., and Iwatsubo, T. (2010) Functional analysis of the transmembrane domains of presenilin 1: Participation of transmembrane domains 2 and 6 in the formation of initial substrate-binding site of  $\gamma$ -secretase. *J. Biol. Chem.* 285, 19738–19746.
- (20) Herreman, A., Serneels, L., Annaert, W., Collen, D., Schoonjans, L., and De Strooper, B. (2000) Total inactivation of  $\gamma$ -secretase activity in presenilin-deficient embryonic stem cells. *Nat. Cell Biol.* 2, 461–462.
- (21) Kitamura, T., Koshino, Y., Shibata, F., Oki, T., Nakajima, H., Nosaka, T., and Kumagai, H. (2003) Retrovirus-mediated gene transfer and expression cloning: powerful tools in functional genomics. *Exp. Hematol.* 31, 1007–1014.
- (22) Hayashi, I., Takatori, S., Urano, Y., Miyake, Y., Takagi, J., Sakata-Yanagimoto, M., Iwanari, H., Osawa, S., Morohashi, Y., Li, T., Wong, P. C., Chiba, S., Kodama, T., Hamakubo, T., Tomita, T., and Iwatsubo, T. (2012) Neutralization of the  $\gamma$ -secretase activity by monoclonal antibody against extracellular domain of nicastrin. *Oncogene* 31, 787–798.
- (23) Tomita, T., Takikawa, R., Koyama, A., Morohashi, Y., Takasugi, N., Saido, T. C., Maruyama, K., and Iwatsubo, T. (1999) C terminus of presenilin is required for overproduction of amyloidogenic A $\beta$ 42 through stabilization and endoproteolysis of presenilin. *J. Neurosci.* 19, 10627–10634.
- (24) Isoo, N., Sato, C., Miyashita, H., Shinohara, M., Takasugi, N., Morohashi, Y., Tsuji, S., Tomita, T., and Iwatsubo, T. (2007) A $\beta$ 42 overproduction associated with structural changes in the catalytic pore of  $\gamma$ -secretase: Common effects of Pen-2 N-terminal elongation and fenofibrate. *J. Biol. Chem.* 282, 12388–12396.
- (25) Thinakaran, G., Regard, J. B., Bouton, C. M., Harris, C. L., Price, D. L., Borchelt, D. R., and Sisodia, S. S. (1998) Stable association of presenilin derivatives and absence of presenilin interactions with APP. *Neurobiol. Dis.* 4, 438–453.
- (26) Hayashi, I., Urano, Y., Fukuda, R., Isoo, N., Kodama, T., Hamakubo, T., Tomita, T., and Iwatsubo, T. (2004) Selective reconstitution and recovery of functional  $\gamma$ -secretase complex on budded baculovirus particles. *J. Biol. Chem.* 279, 38040–38046.
- (27) Morohashi, Y., Hatano, N., Ohya, S., Takikawa, R., Watabiki, T., Takasugi, N., Imaizumi, Y., Tomita, T., and Iwatsubo, T. (2002) Molecular cloning and characterization of CALP/KChIP4, a novel EF-hand protein interacting with presenilin 2 and voltage-gated potassium channel subunit Kv4. *J. Biol. Chem.* 277, 14965–14975.
- (28) Takahashi, Y., Hayashi, I., Tominari, Y., Rikimaru, K., Morohashi, Y., Kan, T., Natsugari, H., Fukuyama, T., Tomita, T., and Iwatsubo, T. (2003) Sulindac sulfide is a noncompetitive  $\gamma$ -secretase inhibitor that preferentially reduces A $\beta$ 42 generation. *J. Biol. Chem.* 278, 18664–18670.
- (29) Tomita, T., Maruyama, K., Saido, T. C., Kume, H., Shinozaki, K., Tokuhira, S., Capell, A., Walter, J., Grunberg, J., Haass, C., Iwatsubo, T., and Obata, K. (1997) The presenilin 2 mutation (N141I) linked to familial Alzheimer disease (Volga German families) increases the secretion of amyloid  $\beta$  protein ending at the 42nd (or 43rd) residue. *Proc. Natl. Acad. Sci. U.S.A.* 94, 2025–2030.
- (30) Tomita, T., Watabiki, T., Takikawa, R., Morohashi, Y., Takasugi, N., Kopan, R., De Strooper, B., and Iwatsubo, T. (2001) The first proline of PALP motif at the C terminus of presenilins is obligatory for stabilization, complex formation, and  $\gamma$ -secretase activities of presenilins. *J. Biol. Chem.* 276, 33273–33281.
- (31) Tomita, T., Tanaka, S., Morohashi, Y., and Iwatsubo, T. (2006) Presenilin-dependent intramembrane cleavage of ephrin-B1. *Mol. Neurodegener.* 1, 2.
- (32) Suzuki, K., Hayashi, Y., Nakahara, S., Kumazaki, H., Prox, J., Horiuchi, K., Zeng, M., Tanimura, S., Nishiyama, Y., Osawa, S., Sehara-Fujisawa, A., Saftig, P., Yokoshima, S., Fukuyama, T., Matsuki, N., Koyama, R., Tomita, T., and Iwatsubo, T. (2012) Activity-dependent proteolytic cleavage of neuroligin-1. *Neuron* 76, 410–422.
- (33) Kan, T., Tominari, Y., Morohashi, Y., Natsugari, H., Tomita, T., Iwatsubo, T., and Fukuyama, T. (2003) Solid-phase synthesis of photoaffinity probes: Highly efficient incorporation of biotin-tag and cross-linking groups. *Chem. Commun.*, 2244–2245.
- (34) Ohki, Y., Higo, T., Uemura, K., Shimada, N., Osawa, S., Berezovska, O., Yokoshima, S., Fukuyama, T., Tomita, T., and Iwatsubo, T. (2011) Phenylpiperidine-type  $\gamma$ -secretase modulators target the transmembrane domain 1 of presenilin 1. *EMBO J.* 30, 4815–4824.
- (35) Tarassishin, L., Yin, Y. I., Bassit, B., and Li, Y. M. (2004) Processing of Notch and amyloid precursor protein by  $\gamma$ -secretase is spatially distinct. *Proc. Natl. Acad. Sci. U.S.A.* 101, 17050–17055.
- (36) Luistro, L., He, W., Smith, M., Packman, K., Vilenchik, M., Carvajal, D., Roberts, J., Cai, J., Berkofsky-Fessler, W., Hilton, H., Linn, M., Flohr, A., Jakob-Rotne, R., Jacobsen, H., Glenn, K., Heimbrook, D., and Boylan, J. F. (2009) Preclinical profile of a potent  $\gamma$ -secretase inhibitor targeting notch signaling with in vivo efficacy and pharmacodynamic properties. *Cancer Res.* 69, 7672–7680.
- (37) Micchelli, C. A., Esler, W. P., Kimberly, W. T., Jack, C., Berezovska, O., Kornilova, A., Hyman, B. T., Perrimon, N., and Wolfe, M. S. (2003)  $\gamma$ -Secretase/presenilin inhibitors for Alzheimer's disease phenocopy Notch mutations in Drosophila. *FASEB J.* 17, 79–81.
- (38) Kornilova, A. Y., Bihel, F., Das, C., and Wolfe, M. S. (2005) The initial substrate-binding site of  $\gamma$ -secretase is located on presenilin near the active site. *Proc. Natl. Acad. Sci. U.S.A.* 102, 3230–3235.
- (39) Morohashi, Y., Kan, T., Tominari, Y., Fuwa, H., Okamura, Y., Watanabe, N., Sato, C., Natsugari, H., Fukuyama, T., Iwatsubo, T., and Tomita, T. (2006) C-terminal fragment of presenilin is the molecular target of a dipeptidic  $\gamma$ -secretase-specific inhibitor DAPT (N-[N-(3,5-difluorophenacetyl)-L-alanyl]-S-phenylglycine t-butyl ester). *J. Biol. Chem.* 281, 14670–14676.
- (40) Baker, R. P., Young, K., Feng, L., Shi, Y., and Urban, S. (2007) Enzymatic analysis of a rhomboid intramembrane protease implicates transmembrane helix 5 as the lateral substrate gate. *Proc. Natl. Acad. Sci. U.S.A.* 104, 8257–8262.
- (41) Bondar, A. N., del Val, C., and White, S. H. (2009) Rhomboid protease dynamics and lipid interactions. *Structure* 17, 395–405.
- (42) Zhang, X., Hoey, R. J., Lin, G., Koide, A., Leung, B., Ahn, K., Dolios, G., Paduch, M., Ikeuchi, T., Wang, R., Li, Y. M., Koide, S., and Sisodia, S. S. (2012) Identification of a tetratricopeptide repeat-like domain in the nicastrin subunit of  $\gamma$ -secretase using synthetic antibodies. *Proc. Natl. Acad. Sci. U.S.A.* 109, 8534–8539.
- (43) Filipovic, A., Gronau, J. H., Green, A. R., Wang, J., Vallath, S., Shao, D., Rasul, S., Ellis, I. O., Yague, E., Sturge, J., and Coombes, R. C. (2011) Biological and clinical implications of nicastrin expression in invasive breast cancer. *Breast Cancer Res. Treat.* 125, 43–53.
- (44) Gandhi, C. S., Clark, E., Loots, E., Pralle, A., and Isacoff, E. Y. (2003) The orientation and molecular movement of a K<sup>+</sup> channel voltage-sensing domain. *Neuron* 40, 515–525.
- (45) Hazelbauer, G. L., and Lai, W. C. (2010) Bacterial chemoreceptors: Providing enhanced features to two-component signaling. *Curr. Opin. Microbiol.* 13, 124–132.



- (46) Moller, J. V., Nissen, P., Sorensen, T. L., and le Maire, M. (2005) Transport mechanism of the sarcoplasmic reticulum  $\text{Ca}^{2+}$ -ATPase pump. *Curr. Opin. Struct. Biol.* 15, 387–393.
- (47) Spijker, P., Vaidehi, N., Freddolino, P. L., Hilbers, P. A., and Goddard, W. A., III (2006) Dynamic behavior of fully solvated  $\beta_2$ -adrenergic receptor, embedded in the membrane with bound agonist or antagonist. *Proc. Natl. Acad. Sci. U.S.A.* 103, 4882–4887.
- (48) Hino, T., Arakawa, T., Iwanari, H., Yurugi-Kobayashi, T., Ikeda-Suno, C., Nakada-Nakura, Y., Kusano-Arai, O., Weyand, S., Shimamura, T., Nomura, N., Cameron, A. D., Kobayashi, T., Hamakubo, T., Iwata, S., and Murata, T. (2012) G-protein-coupled receptor inactivation by an allosteric inverse-agonist antibody. *Nature* 482, 237–240.
- (49) Rasmussen, S. G., Choi, H. J., Fung, J. J., Pardon, E., Casarosa, P., Chae, P. S., Devree, B. T., Rosenbaum, D. M., Thian, F. S., Kobilka, T. S., Schnapp, A., Konetzki, I., Sunahara, R. K., Gellman, S. H., Pautsch, A., Steyaert, J., Weis, W. I., and Kobilka, B. K. (2011) Structure of a nanobody-stabilized active state of the  $\beta(2)$  adrenoceptor. *Nature* 469, 175–180.